

Accepted Manuscript

Urban flood modelling combining cellular automata framework with semi-implicit finite difference numerical formulation

U.C. Nkwunonwo, Malcolm Whitworth, Brian Baily



PII: S1464-343X(18)30339-X

DOI: <https://doi.org/10.1016/j.jafrearsci.2018.10.016>

Reference: AES 3353

To appear in: *Journal of African Earth Sciences*

Received Date: 2 November 2016

Revised Date: 17 September 2018

Accepted Date: 30 October 2018

Please cite this article as: U.C. Nkwunonwo, Malcolm Whitworth, Brian Baily, Urban flood modelling combining cellular automata framework with semi-implicit finite difference numerical formulation, *Journal of African Earth Sciences* (2018), doi: 10.1016/j.jafrearsci.2018.10.016

This is a PDF file of an unedited manuscript that has been accepted for publication. As a service to our customers we are providing this early version of the manuscript. The manuscript will undergo copyediting, typesetting, and review of the resulting proof before it is published in its final form. Please note that during the production process errors may be discovered which could affect the content, and all legal disclaimers that apply to the journal pertain.

1 Urban flood modelling combining cellular automata framework with semi-
2 implicit finite difference numerical formulation

3
4 Nkwunonwo, U.C.^{1,2}, Whitworth, Malcolm², Baily, Brian³

5
6 ¹Department of Geoinformatics and Surveying, University of Nigeria, Enugu Campus.

7 ²School of Earth and Environmental Sciences, University of Portsmouth, UK.

8 ³Department of Geography, University of Portsmouth, UK.
9

10
11 **Abstract**

12
13 Urban flooding is increasingly pervasive, with dreadful impacts on people and development
14 assets. Whilst the frequency of occurrence of this hazard, mainly from pluvial events, is of
15 fundamental importance in climate change and earth sciences research, the severity of its
16 impacts motivates major debates within the context of flood risk management and
17 sustainable urban development. The present study focuses on the development of a novel
18 flood model, as a contribution to meeting the challenges of flood risk assessment within
19 data poor urban areas such as in Nigeria. The new model combines the full functionality of
20 cellular automata (CA) framework with a semi-implicit finite difference numerical scheme
21 (SIFDS), whilst the resulting algorithms were programmed within MATLABTM programming
22 platform. In this study, computation complexity and distributed topographic data
23 requirement, both which are associated with flood modelling, and which tend to present a
24 major limitation to flood modelling in the developing countries (DCs) are being addressed. A
25 highly urbanized area within the Lagos metropolis of Nigeria was chosen as a case study to
26 validate the model and to simulate the July 10th 2011 flooding event. A 2-m horizontal
27 resolution LiDAR DEM, published Manning's friction coefficients and rainfall intensity, were
28 used as data inputs into the new flood model. Simulated results compared well with actual
29 flooding inundations, reported by urban residents, and detailed in some literature and by
30 the media. The Pearson correlation coefficient (r) between predicted flood depth and
31 estimated values is 0.968. It is expected that the challenges of urban flooding in Lagos
32 particularly and in the DCs generally will be better addressed if robust, but low-cost flood
33 models are developed and utilized in the assessment of flood damage.
34

35 *Keywords:* Urban flooding, Flood modelling, Flood risk assessment, Cellular automata,
36 Semi-implicit finite difference scheme.
37

38 1. Introduction

39

40 Concerns about widespread urban flooding have increased in recent times, whilst it remains
41 an emerging theme in various research relating to climate change, natural hazards, earth
42 sciences and flood risk management (Cherqui *et al.*, 2015, Anees *et al.*, 2016). During urban
43 flooding, surface water inundates large areas with severe impacts whereby human life is
44 threatened and large sections of the population are displaced from homes and traumatized.
45 At the same time critical infrastructure is destroyed, whilst a myriad of economic activities
46 are disrupted (Kaźmierczak & Cavan, 2011). Climate change with its potential to increase the
47 magnitude and frequency of heavy rainstorms is largely implicated in urban flooding
48 (Djordjević *et al.*, 2011). Poor urban drainage facilities which are easily overwhelmed by
49 excess rainfall and infiltration process which is attenuated by widespread use of impervious
50 surfaces in cities escalate these floods (Zevenbergen *et al.*, 2008; Perales-Momparler *et al.*,
51 2017). Recent flood disasters across the globe show that the severe impacts of urban
52 flooding frequently correlate with high concentrations of human population and associated
53 developments in urban areas. This means that with the rapid growth in global population
54 and the amount of wealth being amassed comes increased human exposure with more and
55 more personal and corporate wealth being placed at risk (Smith, 2013).

56

57 Issues arising from extant discussions in flood risk research suggest the need to identify the
58 various human and environmental agencies of urban flooding and their interactions, as well
59 as to develop robust and more realistic methodologies for assessing and managing flood risk
60 within the context of urban areas. This highlights the importance of flood modelling, to
61 characterize or predict a flooding event in terms of the flood water depth, extent and water
62 flow velocity and produce flood risk maps (Teng *et al.*, 2017). With the growing application
63 of depth-damage functions for economic assessment of flood risk, flood modelling has
64 become a primary research concern, for which significant progress has been made over the
65 years especially in modelling of fluvial and coastal flooding (Costabile & Macchione, 2015).
66 Modelling of urban flooding has arguably not received sufficient attention. There have been
67 several research initiatives towards urban flood modelling, although it seems the increased
68 availability of urban flood models have unrealistic corresponding effects on the growing
69 challenges of urban flooding, especially in developing countries (DCs) (Nkwunonwo *et al.*,
70 2015). Within urban flood modelling research, specific objectives such as representation of
71 urban geomorphology, LiDAR (Light Detection and Ranging) processing tailored to urban
72 flood modelling, paucity of high resolution topographic data, computation effectiveness and
73 model uncertainty are still ongoing debates (Chen *et al.*, 2012; Kim *et al.*, 2018).

74

75 The main aim of the present research is to advance the availability of models for simulating
76 urban flooding. Within this research two specific objectives are being addressed which are
77 computation simplicity and minimum data requirement. Thus, a new flood model, named
78 *GFSP-1 (Geoinformation Flood Simulation Program-1)*, which combines the capability of a
79 semi-implicit finite difference scheme (SIFDS) and cellular automata (CA) framework is being
80 proposed. The model is coded using MATLABTM programming language, and used to
81 simulate the July 10th 2011 flooding of the urban areas of Lagos Nigeria, West Africa. Only
82 digital elevation models (DEM), rainfall intensity and Manning's friction coefficient were
83 used as variables to simulate urban flooding inundation. The authors hypothesize that whilst
84 fragility functions are being widely utilized for economic assessment of flood damage, the
85 development of bespoke models to simulate urban flooding will greatly enhance the use of
86 such functions especially in the DCs.

87 2. Methodology

88 The technical design of *GFSP-1* consists of CA framework and the SIFDS formulation. CA
89 signifies a set of mathematical procedures that solve complex systems on cellular spaces in
90 which time is discrete and a set of universal laws apply (Engelen *et al.*, 1995; Wahle *et al.*,
91 2001). It represents one of the most recent efforts to address the gaps in the science of
92 flood modelling (Cirbus & Podhoranyi, 2013; Liu *et al.*, 2015). The popularity of CA in the
93 physical sciences is linked to the work of Von Newman and Stanislaw Ulam in the 1940s and
94 has since gained significant attention in many research areas to dynamically model systems
95 whose states evolve with respect to time and space (von Neumann, 1951). The relative
96 advantage of CA over other techniques for simulating physical systems is its ability for
97 spatial and temporal discretization (Ghimire *et al.*, 2013). In the context of flood modelling,
98 this advantage is expected to scale down the computation burden associated with physically
99 based numerical models. The CA framework proposed in this research encompasses the
100 four essential features of an ideal CA system. These include; the mesh of cellular space,
101 neighbourhood, transition rules and boundary conditions. CA formulation presented in
102 Ghimire *et al.* (2013) has two additional elements, system state and time step. Time step is
103 an important factor not only for CA framework, to determine the pace at which the model
104 operations progress, but also in the simulation of dynamic systems elsewhere.

105

106 – The mesh of cellular space provides the simulation domain. It is made up of a framework
107 of grids, which define a discrete representation of the geometry involved in the physical
108 phenomenon. Any of the LiDAR data types – digital terrain model (DTM), digital surface
109 model (DSM) and DEM can provide the two-dimensional cellular space for the present
110 CA system. A 2-*m* horizontal resolution LiDAR DEM was used in the test case presented
111 later on, although 3-*m* and 5-*m* resolutions are also applicable.

112

113 – The neighbourhood defines the distance from a given origin of a set of objects or points,
114 within a cellular space. The von Neumann type of neighbourhood was considered in the
115 present CA framework. It consists of five cells with the principal cell located at the
116 center of the mesh and four adjacent cells bounding the cardinal directions (East, West,
117 South, and North). Yamamoto *et al.* (2007) argued that simplicity is a key merit of von
118 Neumann neighbourhood in comparison to Hexagonal and Moore neighbourhood
119 systems.

120

121 – Transition rule(s) consist of a set of principles based on mathematical expressions that
122 direct the CA procedure. The transition rules control how the neighbouring cells interact
123 with each other, and in turn the model performance by dictating what takes place at
124 each stage of the model iteration. In the present CA formation, a set of four transition
125 rules were implemented. They include: rule for adding rainfall into the individual cells
126 and excluding losses especially through infiltration and evapotranspiration, rule - based
127 on Manning's formula (*equation 1*) - to determine the length of time water stays in the
128 cells before distribution, rule - based on *equation 2* - to compute the amount of water to
129 be transferred as flux from the principal cell into neighbouring cell. In actual fact, the
130 hydraulic differences between the principal cell and the neighbouring cells drive water
131 movement. This is the routing scheme for *GFSP-1*, by which water is transferred from
132 the principal cell into whichever neighbouring cell has the lowest elevation. This scheme
133 has the effect of reducing the computation time of the model and allowing water to flow
134 over a variable urban terrain without causing much computation errors to the predicted

values. The final rule controls the minimum water level which each cell can retain. In the present model, water depth ≤ 0.01 is considered zero. By doing this, the model separates flooded cells from empty cells, and thus reflects the concept of wetting and drying which is fundamental in urban flood modelling.

$$V = \frac{h^{\frac{2}{3}} \sqrt{S_f}}{n} \quad (1)$$

$$flux(i, j) = \frac{(principal\ cell(i, j) - neighbour\ cell(i, j))}{neighbour\ cell(i, j)} * water\ in\ principal\ cell \quad (2)$$

Where $V (LT^{-1})$ is the velocity, (L) is the water depth, $flux$ is the rate of change of discharge across a unit area (LT^{-3}) and $S_f (-)$ is the water surface slope, computed using the method proposed in Zevenbergen and Thorne (1987).

- The boundary condition applies to the cells bounding the margins of the mesh of cellular space. Allowing that these border cells do not have a complete neighbourhood system, certain formulations are applied to them. In the present CA, absorptive and reflective boundary conditions (somewhat like Dirichlet boundary condition in a regular numerical modelling, refer to: Bazilevs & Hughes, 2007) were used (see figure 1). The absorptive boundary is a 'one-way permeable boundary in which case water flowing off the boundaries disappears. Reflective boundary condition assumes virtual cells for the missing sides of the boundary cells for all model variables. The values contained in these virtual cells are considered as nullity.

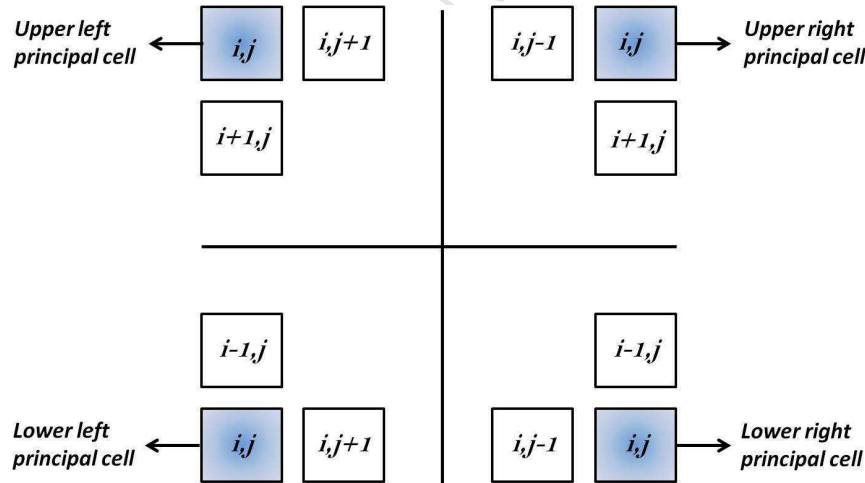
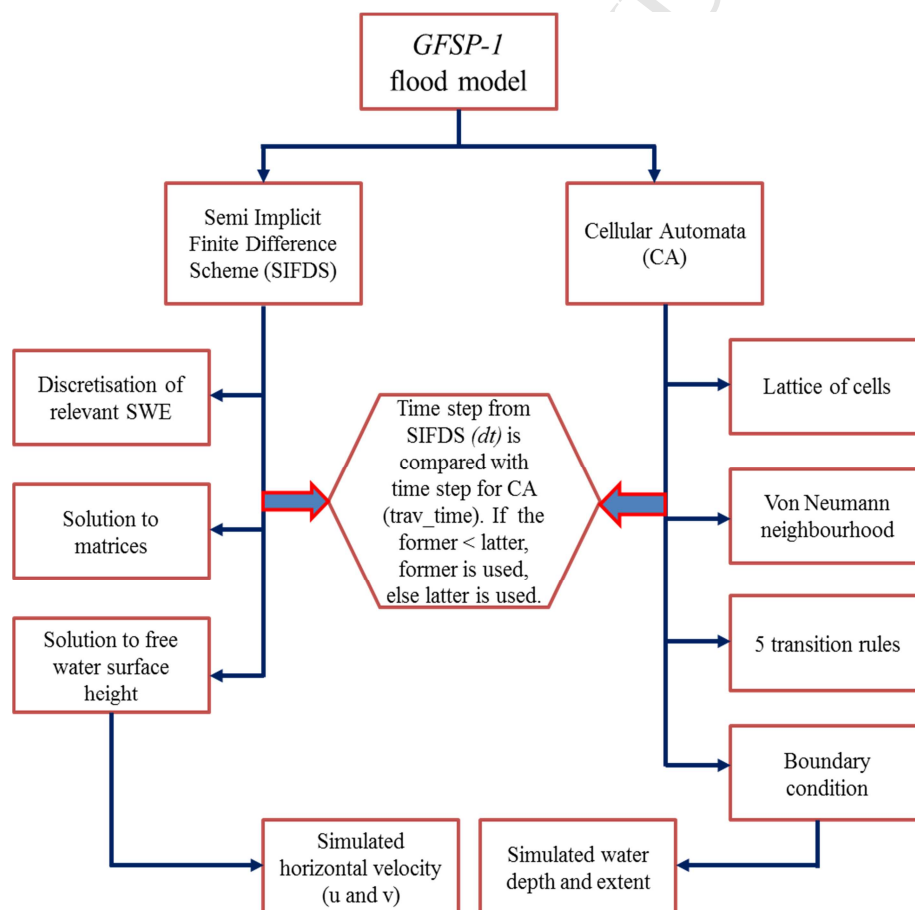


Figure 1: Boundary Condition- the blue-dyed boxes represent the boundary cells, whilst the hollow boxes are the remaining members of the neighbourhood. There are only three cells, which imply an incomplete von Newman neighbourhood at the boundaries.

The SIFDS that couples with CA in the present model is based on the original work of Casulli (1990). It is an attempt to provide a realistic flow solution at a reduced computation cost within the framework of unconditional model stability. Casulli (1990) derived the SIFDS on a staggered grid using a combination of explicit and implicit numerical schemes. The free water surface slope in the momentum equations and the velocity in the continuity equations with friction terms were discretised implicitly. This removes the stability of the model from wave celerity. The other terms in the shallow water equations (SWEs) were

183 discretised explicitly. This method of discretization incorporates the relative advantages of
 184 the explicit and implicit schemes (which are computation cheapness and unconditional
 185 stability respectively) into a single flood simulation model. The resulting SIFDS equations are
 186 shown in Casulli (1990), Casulli and Stelling (2013), Dumbser and Casulli (2013), Dumbser *et*
 187 *al.* (2015).

188
 189 The combination of CA and SIFDS in the present research introduced a dynamic interaction
 190 between two model components to enhance model performance in simulating a typical
 191 urban flooding event. From figure 2, the link between CA and SIFDS determines the time
 192 step or simulation time of the model. Once the model begins to run, an initial time step
 193 (*traverse time*) is computed using Manning's flow formula. This time step is the minimum
 194 that is required to keep the simulated results at a maximum principle (which means not
 195 compromising the stability). Midway through the simulation period, a new time step (∂t)
 196 emerges from the SIFDS. This time step is needed to simulate horizontal velocity
 197 components (u , v) and to keep the model through a complete iteration. At the point of
 198 intersection between the two model components, the time step that emerged from the
 199 SIFDS is compared with the time step initiated at the start of the simulation. The minimum
 200 of the two is then used to advance up to a full iteration, leading to evolution of water depth.



225
 226 Figure 2: Schematics showing the dynamic link between the CA and the SIFDS
 227 in the *GFSP-1* model.

228 Evolution of water depth is the most important stage of the new flood modelling technique,
 229 especially within the CA framework, in which the final water depth and extent for each time
 230 step is updated. In the present flood model, the fluxes into the cells are first summed up for
 231 each time step using *equation 3*. Then the total fluxes are divided by the areas enclosed by

232 the cell (i.e. $dx * dy$) and multiplied by the model time step, using *equation 4*. Ghimire *et al.*
 233 (2013) raised the issue of using a variable cell area to reflect the reduced space occupied by
 234 topographic feature, especially built-up structures, which intervene in the flow path of
 235 water. This idea is logical but it can be difficult to implement. Within the present model, it
 236 may lead to a significant increase in the computation cost since creating new variables,
 237 initializing and updating them within a single iteration can overwhelm the speed of MATLAB
 238 computation. However, the down-gradient flow assumption ensures that water flows
 239 completely around large obstructions, rather than being enclosed and accumulating.

240

$$241 \quad Total\ flux(i,j) = \sum\{influx(i-1,j),influx(i+1,j),influx(i,j-1),influx(i,j+1)\} \quad (3)$$

242

$$243 \quad Water\ depth(i,j) = water\ depth(i,j) + \frac{Totalflux(i,j)}{(dx*dy)} * \Delta t \quad (4)$$

244

245

246

247

Where Δt (T) is the model time step

248 The present model is coded and implemented in MATLABTM which is a powerful, easy to
 249 implement object oriented programming (OOP) language. MATLABTM has several in-built
 250 functions, with capability for modularity and for handling and manipulating matrices (which
 251 are the building block of DEMs). This choice of MATLABTM in this research is an attempt to
 252 advance research towards using the potentials and capabilities of MATLABTM to improve
 253 flood modelling techniques. Programming flood simulation models using MATLABTM is still
 254 an emerging procedure with only few flood models essentially programmed in MATLABTM
 255 (see MOD2-Flow model: Martin & Gorelick, 2005; Kulkarni *et al.*, 2014). As a commercial
 256 programming language, access to end-users in low income societies can be limited.
 257 However, MATLABTM codes can easily be exported and adapted to freely accessible windows
 258 integrated program development environments (IDEs).

259

260

261

3. Model testing and validation using the Lagos case study

3.1. Study area description

262

263

264 Lagos is the largest city in Nigeria, and the second largest in Africa. Its most functional part,
 265 the 'Lagos metropolis', is made up of sixteen local government areas (LGAs) of varying
 266 enumeration sizes. The Lagos metropolis is located in the south western part of Nigeria from
 267 latitude $6^{\circ} 24' N$ to $6^{\circ} 48' N$ and longitude $3^{\circ} 10' E$ to $3^{\circ} 24' E$, enclosing a relatively small land
 268 mass, just about $1100\ km^2$ (see figure 3). The metropolis is a densely populated urban area
 269 with an estimated population of over 21 million people (LSG, 2012). The city is annually
 270 threatened by flooding from excess rainfall, which was not infiltrated due to much
 271 impervious surfaces, nor evacuated by available drainage facilities. The July 2011 event
 272 which was triggered by heavy rainfall that lasted two days remains historic in terms of its
 273 large scale impacts on human population and development assets. The meteorological data
 274 for the event suggests that approximately 463 mm of rainfall was recorded for the month,
 275 although most of the rain fell within 17 hours of the 10th day (IFRC, 2011; Adelekan, 2015).
 276 Losses estimated at millions of USD were incurred from the event. Unfortunately, the lack of
 277 data relating to flood depth and extent was a major constraint to *GFSP-1* model validation.
 278 Although, there have been major flood management efforts, flooding and its threats are still
 279 important problems, especially among the poor urban communities who lack the capacity to

280 cope and the means to adapt with the challenges (Adelekan, 2010, Nkwunonwo *et al.*,
 281 2016).

282

283

284

285

286

287

288

289

290

291

292

293

294

295

296

297

298

299

300

301

302

303

304 3.2. Model validation datasets

305

306

307

308

309

310

311

312

313

314

315

316

317

318

319

320

321

322

323

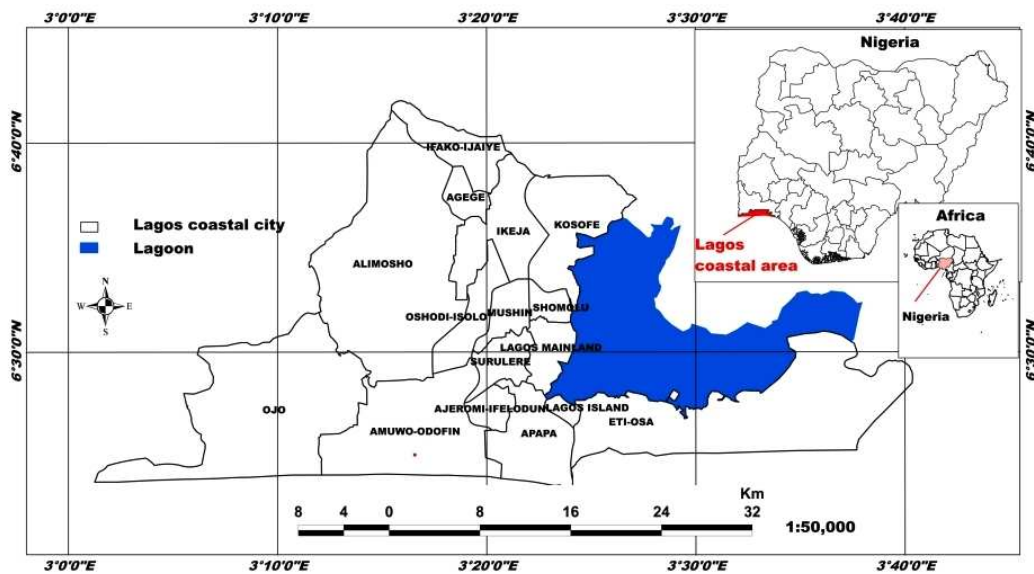


Figure 3: The Lagos metropolis of Nigeria (Inset showing Africa and Nigeria).

300

301

302

303

304 3.2. Model validation datasets

305

306

307

308

309

310

311

312

313

314

315

316

317

318

319

320

321

322

323

The key data used in validating *GFSP-1* is the LiDAR DEM, which within the present test case, covers some places within Eti-Osa and Lagos Island LGAs. The Lagos LiDAR data which comes in the original (.las) format was acquired from GIS section of the Lagos state office of Lands and Survey. Lagos is the only region in Nigeria that has acquired such a dataset. Each tile forms a regular polygon dense of DSM, measuring 500 meters by 500 meters (see figure 4). The horizontal and vertical resolutions are 1m respectively (although each tile was subsequently resampled to a 2-m horizontal resolution to ease the computation burden of *GFSP-1*). Each tile cost about twenty thousand Nigerian naira (i.e. £90 using the 2013 exchange rate). It was reported by Nkwunonwo *et al.* (2016) that the cost of acquiring these datasets remains a significant constraint to flood modelling in Lagos. However, in the present research, 32 tiles were acquired for this research, to delineate flood hazard on a relatively wider spatial extent.

These 32 tiles are unable to facilitate a nuanced understanding of the elevation differences of the study area, and how they affect the simulation results. Thus, a 35-meter elevation map of Lagos, which displays range of elevation with different colours, shown in figure 4a, will be superimposed on the simulated results. The map was generated using elevation data from NASA's 90m horizontal resolution SRTM data.

324
325
326
327
328
329
330
331
332
333
334
335
336
337
338
339
340

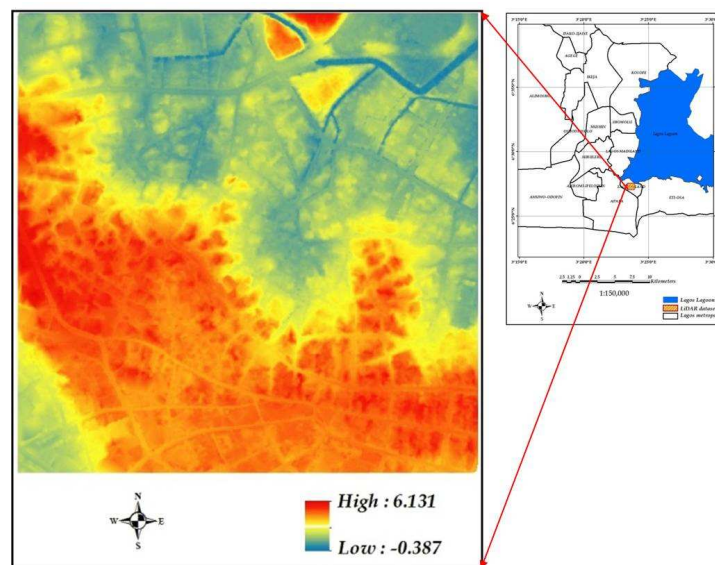


Figure 4: one tile of the 1-m horizontally-spaced point cloud LiDAR DSM of the study area.

342

343
344
345
346
347
348
349
350
351
352
353
354
355
356
357
358
359
360
361
362
363
364
365
366
367
368

The rainfall datasets were acquired from NIMET. Two months rainfall data at a daily amount sampling rate were acquired (see table 1). To obtain effective rainfall intensity for the simulation, average of respective intensities was taken (a solution that is being proposed in the literature) (for example Chen, 1983). For the present model, it is assumed that effective rainfall intensity disaggregates the daily rainfall amounts to hourly measures, so that simulated flood inundation can be characterised over the recorded duration of the rainfall (Wójcik & Buishand, 2003). Using this approach, the effective rainfall amount was calculated to be 0.65 mm/hr. Abstractions and other losses were not considered in the present simulation due to lack of data relating to them. A roughness coefficient of 0.02 was adopted from published values in Chow *et al.* (1988).

Table 1: Rainfall data for the July 11th 2011 flooding event. Source: NIMET

Date	July	August	Date	July	August	Date	July	August
1	2.5	0.0	12	0.0	0.1	23	0.0	0.0
2	50.6	44.3	13	8.1	2.6	24	0.0	0.0
3	1.3	0.0	14	11.1	0.0	25	0.1	0.1
4	0.0	1.4	15	0.1	0.0	26	0.1	1.6
5	25.8	0.1	16	1.4	0.0	27	0.0	4.0
6	2.5	4.2	17	49.2	0.0	28	4.0	2.0
7	14.6	0.0	18	0.0	0.0	29	0.0	0.0
8	0.2	3.4	19	0.0	0.0	30	3.1	4.9
9	0.8	0.0	20	0.0	0.0	31	0.0	14.5
10	252.4	0.0	21	1.2	0.0			
11	34.4	0.0	22	0.0	4.0	TOTAL	463.5	87.2

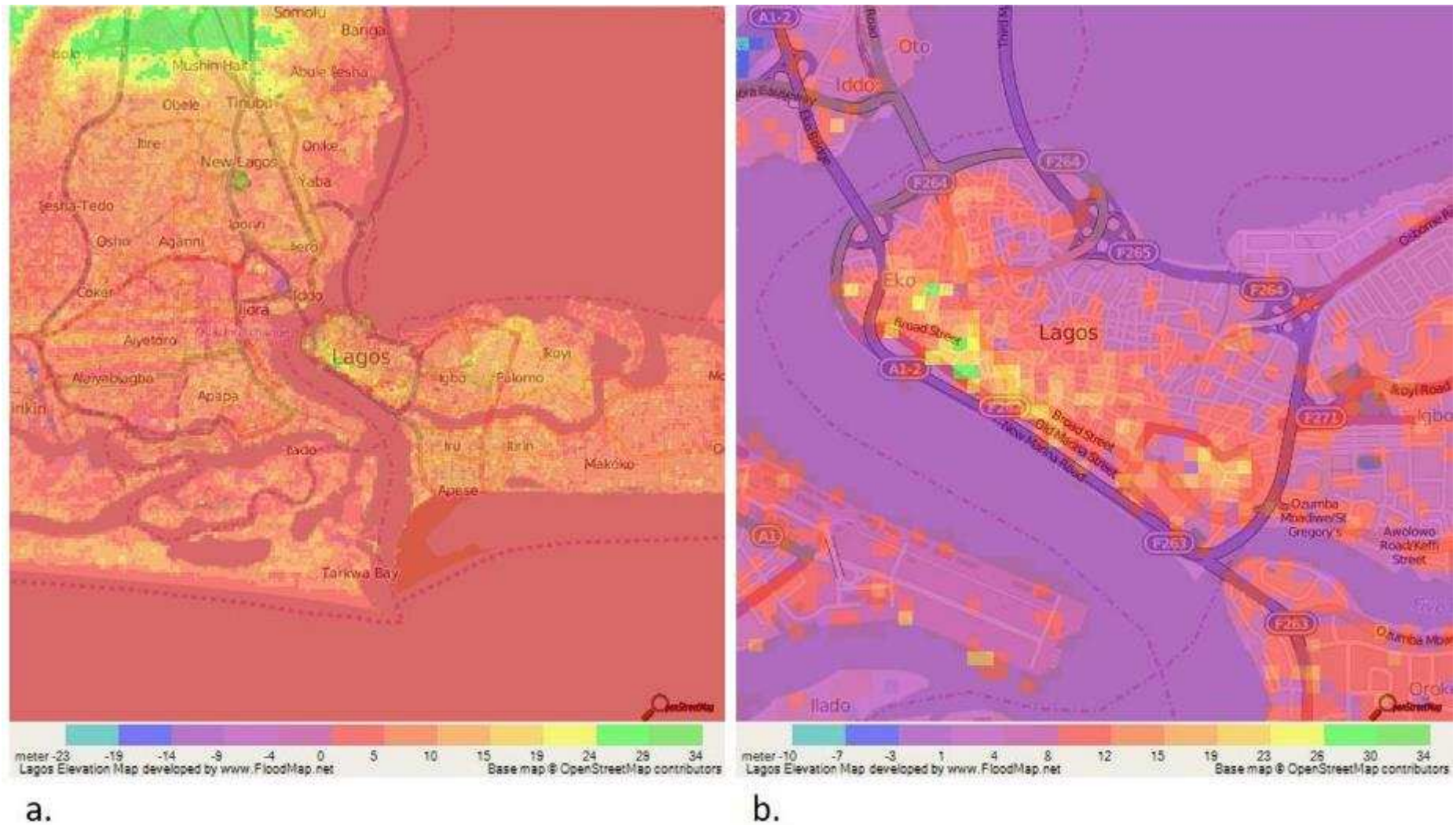


Figure 4a: 35-meter elevation map of Lagos, which displays range of elevation with different colours. The map was generated using elevation data from NASA's 90m resolution SRTM data (www.floodmap.net). (a) Elevation map for Lagos area. (b) Elevation map for part of the study area.

405 An on-site survey was conducted over the areas covered by the acquired Lagos LiDAR data.
406 During this survey, thirty flood inundation locations were identified, whilst up to fifty
407 anonymous residents were questioned (thirty of which has been used in model validation),
408 and this provided detailed eye witnesses' testimonies of the flooding event (see table 2).
409 The geographical coordinates (Longitudes and Latitudes) of these locations were measured
410 with the help of a handheld Global Positioning System (GPS) gadget. Photographs were
411 taken of the physically perceived flooding inundation.

412

413 3.3. Model validation procedure

414

415 In the present research, quantitative information extracted from photographs has been
416 used to validate *GFSP-1*. This is due to the lack of measured flood water, coupled with lack
417 of funds to acquire synthetic aperture radar (SAR) satellite data which can be analyzed to
418 extract water levels for the historical flooding being simulated. There is ample evidence to
419 show the increasing utility of social media data such as Flickr, twitter, newspaper reports,
420 online photographs, etc., to validate flood model in situations where authoritative and field-
421 based datasets are lacking (Latonero & Shklovski, 2011; Alexander, 2014; de Albuquerque *et*
422 *al.*, 2015; Smith *et al.*, 2015). Liu *et al.* (2015) used videos acquired from street-monitoring
423 closed-circuit television (CCTV) to validate a 2-D flood model for city emergency
424 management. Fohringer *et al.* (2015) treated the issue of accuracy and reliability of social
425 media-based information from the point of view of expediency. The study argues that the
426 growing need for flood inundation data should not overrule data availability with its
427 reliability. Thus suitable data should be defined and used on the basis of availability,
428 enabling the flexibility for updating or replacement by more authoritative datasets, and this
429 is the driving principle of the model validation carried out in the present research.

430

431 Social media data such as photographs show contextual information and situational
432 relationship between water level and some parts of the environment such as buildings,
433 submerged cards, and pavements. These enable the estimation of water depth depending
434 on the extent to which the parts of the environment delineated by the photographs have
435 been submerged by flood water. In estimating the flood water depth, the present research
436 adopts the method of visual inspection of the photographs, in line with the study by
437 Fohringer *et al.* (2015), which produce inundation maps of on the basis of photographs that
438 were visually inspected to estimate inundation depth of the recent 2013 flooding in Dresden
439 Germany. This method which is also applicable in photogrammetric and analogue remote
440 sensing image interpretation is an expert elicitation technique which uses image properties
441 such as shape, size, situation, shadow, etc., to estimate information from photographs.

442

443

444

445

446

447

448

449

450

451

452

453

454
455

Table 2: Locations identified based on media reports and living evidence

S/No	LGA	Specific location	Longitude (Decimal degree)	Latitude (Decimal degree)	Source
P1	Lagos-Island	Balogun street	3.384	6.455	Vanguard
P2	Lagos-Island	Broad street	3.385	6.454	Vanguard
P 3	Lagos-Island	Macaulay street	3.397	6.453	Nkwunonwo <i>et al.</i> , (2016)
P 4	Lagos-Island	Idumago avenue	3.390	6.460	Eye witness
P 5	Eti-Osa	Osborne phase 6	3.411	6.460	Eye witness
P 6	Eti-Osa	Dolphin Estate	3.413	6.456	Vanguard
P 7	Eti-Osa	Federal Secretariat	3.413	6.456	Vanguard
P 8	Eti-Osa	Dolphin Estate	3.432	6.458	Street Journal
P 9	Eti-Osa	Obalande	3.432	6.444	Etuonovbe, (2011)
P 10	Eti-Osa	Falomo	3.421	6.443	Akanni & Bilesanmi, (2011)
P 11	Eti-Osa	Ikoyi	3.431	6.455	Ajibade <i>et al.</i> , (2013)
P 12	Eti-Osa	Ikoyi	3.431	6.446	IFRC, (2011)
P 13	Eti-Osa	Ikoyi	3.436	6.459	Etuonovbe, (2011)
P 14	Eti-Osa	Ikoyi	3.442	6.444	Vanguard
P 15	Eti-Osa	Ikoyi	3.447	6.461	PM news
P 16	Eti-Osa	Ikoyi	3.447	6.452	Etuonovbe, (2011)
P 17	Eti-Osa	Ikoyi	3.449	6.444	Nairaland forum
P 18	Eti-Osa	Ikoyi	3.444	6.440	CNNiReport
P 19	Eti-Osa	Castle estate	3.459	6.430	Eye witness
P 20	Eti-Osa	Castle estate	3.457	6.425	Eye witness
P 21	Eti-Osa	Castle estate	3.450	6.428	Eye witness
P 22	Eti-Osa	Castle estate	3.439	6.433	Eye witness
P 23	Eti-Osa	Victoria Island	3.437	6.427	Aderogba (2012)
P 24	Eti-Osa	Victoria Island	3.431	6.434	Ajibade <i>et al.</i> , (2013)
P 25	Eti-Osa	Victoria Island	3.428	6.439	Aderogba, (2012)
P 26	Eti-Osa	Victoria Island	3.429	6.431	Nkwunonwo <i>et al.</i> , (2016)
P 27	Eti-Osa	Victoria Island	3.419	6.430	IFRC, 2011
P 28	Eti-Osa	Victoria Island	3.410	6.435	IFRC, 2011
P 29	Eti-Osa	Victoria Island	3.413	6.428	Aderogba (2012)
P 30	Eti-Osa	Victoria Island	3.411	6.424	Oyinloye (2013)

456
457
458
459
460
461
462
463
464
465
466
467
468
469
470
471
472
473
474
475
476
477

In applying this technique to the present research, six photographic images (figure 5) of July 10th 2011 Lagos flooding, carefully selected from online sources, were used to estimate ranges of flood water depth. To extract the water depths from these photographs, the present research considered the assumption that a true value is unrealistic, and that redundant measurements are often made, and average taken, to obtain the most probable value (*mpv*). To implement this assumption, a range of values are estimated for water depth, considering the extent to which environmental feature have been submerged. For example if an adult is trapped in flood water up to the knee level, then the water depth is estimated to lie between 0.5m and 0.7m. When a car is submerged up to the bonnet, water depth is estimated to lie between 0.7m and 0.9m. Submerged buildings are difficult in this regard, whilst water depth estimated within the interiors of houses different markedly from that estimated outside the building compound. In the present research, only the outside flood water is considered. With the knowledge that many houses measure up to 1m from the floor to the window, water depth can be estimated to lie between 1.5m and 2m for a building that has been submerged up to the top lintel. When a building is completely submerged, water depth is estimated to lie between 2.5m and above.

478
479
480
481
482
483
484
485
486
487
488
489
490
491
492
493
494
495
496
497
498
499
500
501
502
503
504
505
506
507
508
509
510
511
512
513
514
515
516
517
518
519
520
521
522
523
524
525
526



Figure 5: Photographic images of July 11th 2011 Lagos flooding. *GFSP-1* model was validated against water depth values estimated from these photographs.

GFSP-1 provides a link with the user through an input file (input.txt) which must be located in the same folder as the DEM and the model code. The input file is editable and allows the user to enter the DEM name, rainfall intensity, and the assumed Manning's Coefficient value. Initial and final times of simulation are also entered in the input file. The model requires MATLABTM program to be pre-installed and running on computer system. To enhance the computation speed the model, a minimum processing speed of 2.0GHz along with a minimum RAM of 2GB will be desirable.

Once the model begins to run, effective rainfall is assumed to land uniformly on the domain. Hydrological losses entered into the input file are accounted for. The water depth is outputted at the interval based on the user's specification. This is to enable the end-user to have a closer idea of the time-variant flood water depth and extent. In the test cases reported later, water depth is output at 30 minutes, 2 hours, 5 hours, 8 hours, 11 hours, 14 and 17 hours epochs. Some models such as the LISFLOOD-FP specifies a regular interval, for example 10 minutes to output water depth, which means that on a simulation that will last two hours, twelve outputs of simulated flood water depth and extent are expected.

4. Results and Discussion

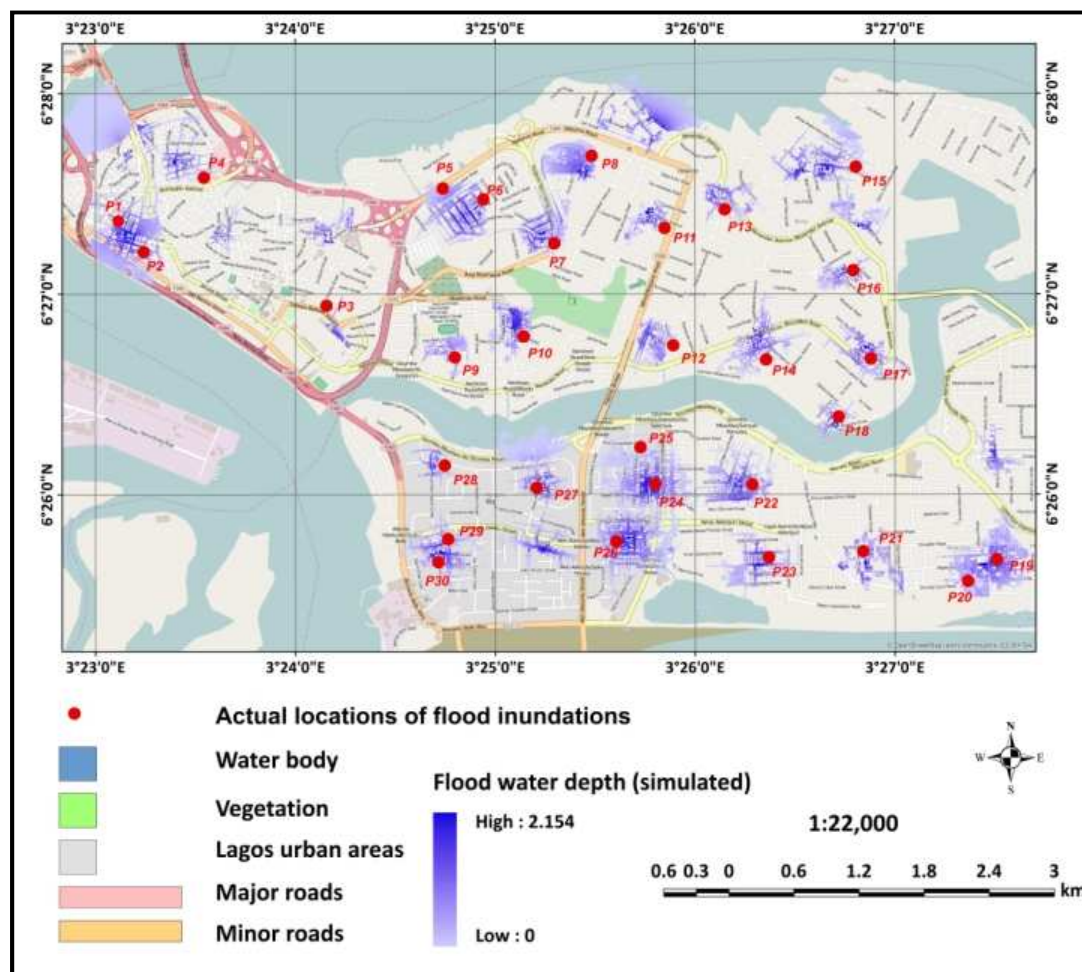


Figure 6: Simulated flooding inundation mapped against actual inundation locations based on secondary sources and eye witness evidence of the July 2011 flooding in Lagos.

From figure 6 above, it can be seen that within the chosen area, *GFSP-1* simulated flood inundations in locations that matched the actual locations of inundation, following the 2011 flooding event. Only *P3*, an area known as Onikan within Lagos-Island was wrongly predicted, as there was no evidence of flood inundation there. To critically assess the performance of *GFSP-1*, and to understand the true impact of the 2011 in terms of spatial and temporal flow variability within the case study, six locations were selected and studied. These locations are spatially distributed within Lagos-Island, Victoria Island, Dolphin estate, and Castle field estate. Results obtained from simulating the 2011 flooding event in these locations are shown in figures 7-12.

This figure was intersected with the section of the elevation map showing the Lagos Island part of the study area. The resulting map (figure 6a) indicates that *GFSP-1* simulated flooding at locations having lower elevations within the study area. This follows the routing scheme which transfers water to a neighbouring cell with elevation value lower than the rest of the cells within a specified neighbourhood system.

574 figure 6a

575

576

577

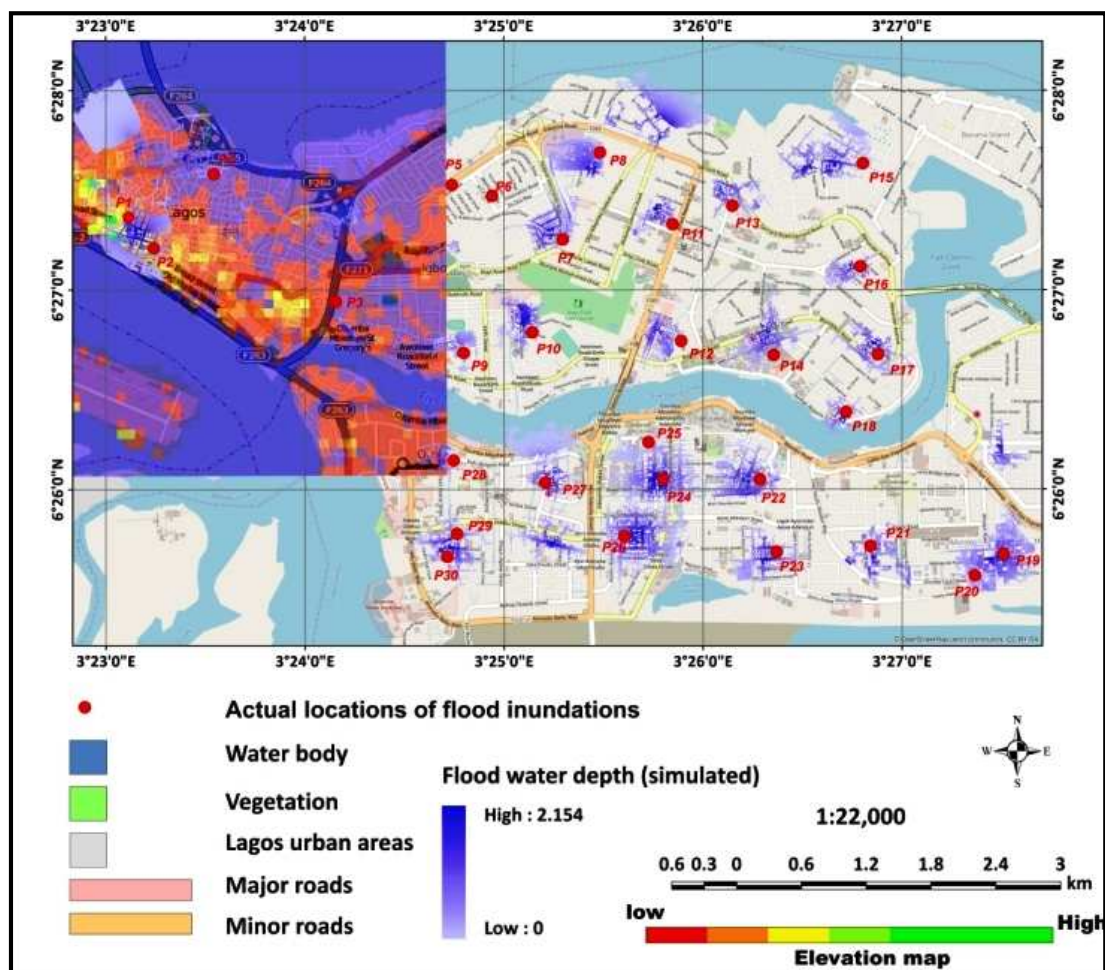
578

579

580

581

582



583

Figure 6a: Simulated flooding inundation intersected with a part of the SRTM elevation map.

584
585
586
587
588
589
590
591
592
593
594
595
596
597
598
599
600
601
602
603
604
605
606
607
608
609
610
611
612
613
614
615
616
617
618
619
620
621
622
623
624
625
626
627
628
629
630
631
632

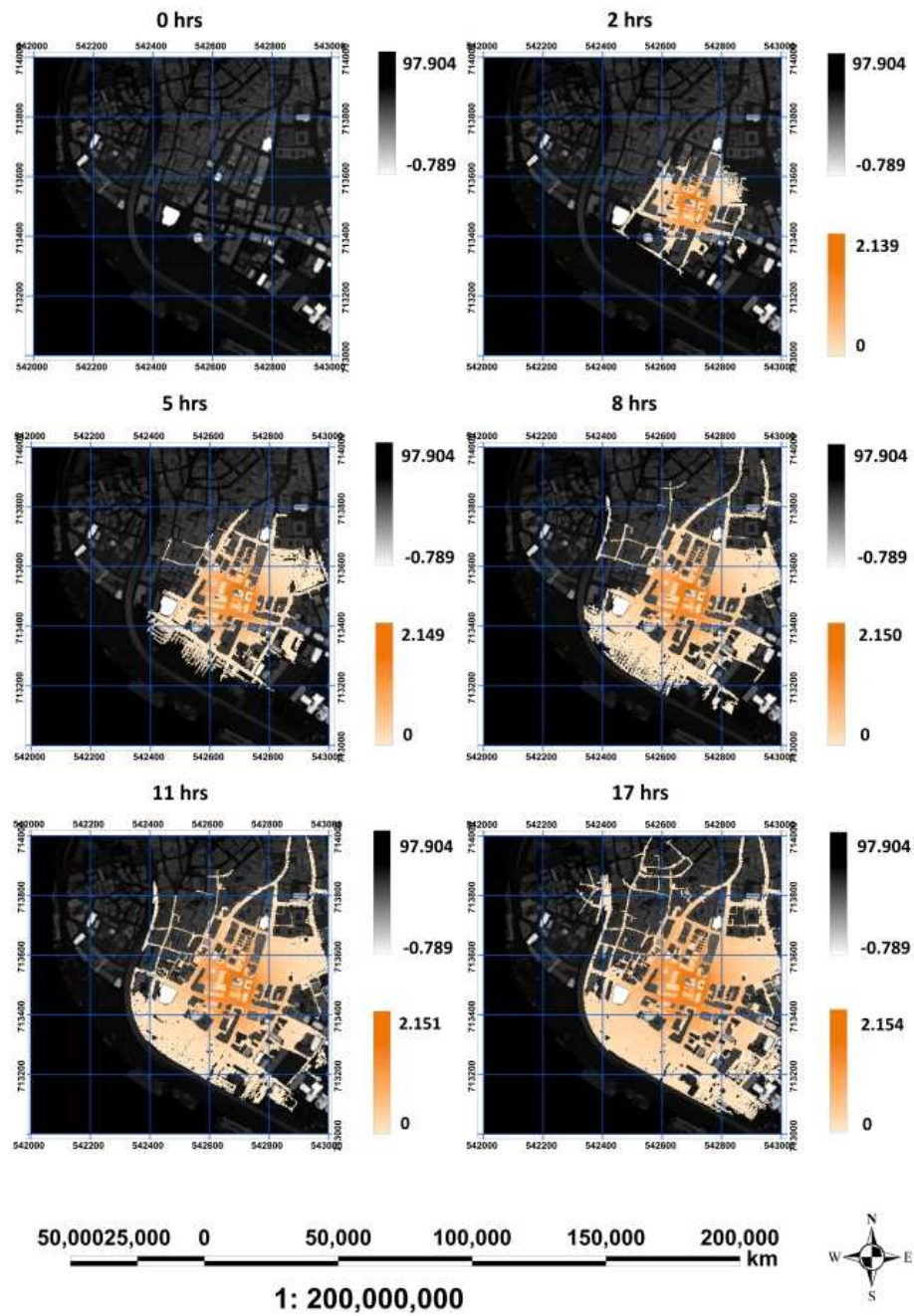


Figure 7: Simulated water depth at Broad and Balogun Street areas, Lagos Island

633
634
635
636
637
638
639
640
641
642
643
644
645
646
647
648
649
650
651
652
653
654
655
656
657
658
659
660
661
662
663
664
665
666
667
668
669
670
671
672
673
674
675
676
677
678
679
680
681
682
683
684

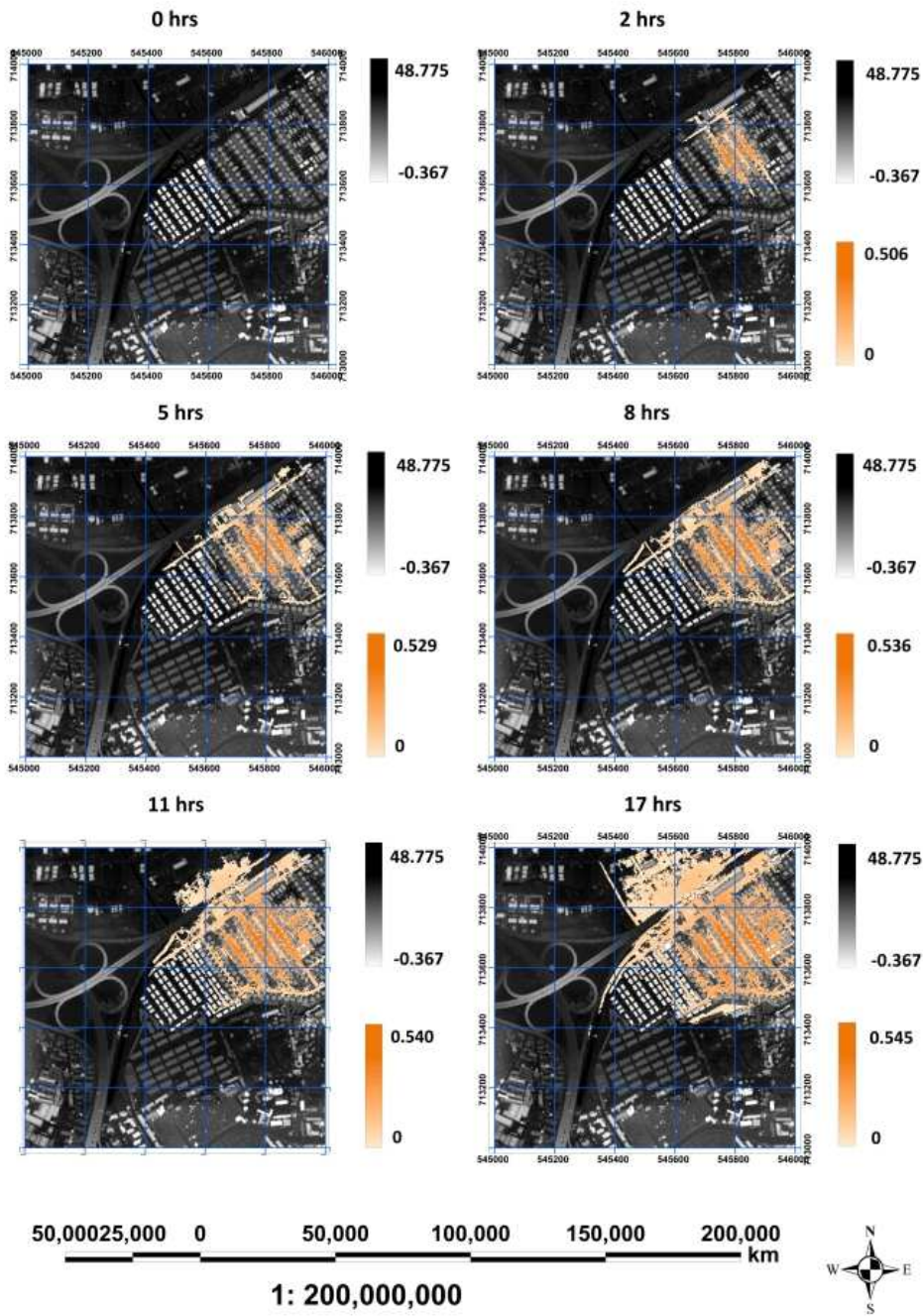


Figure 8: Simulated water depth at Dolphin estate

685
686
687
688
689
690
691
692
693
694
695
696
697
698
699
700
701
702
703
704
705
706
707
708
709
710
711
712
713
714
715
716
717
718
719
720
721
722
723
724
725
726
727
728
729
730
731
732
733
734
735
736

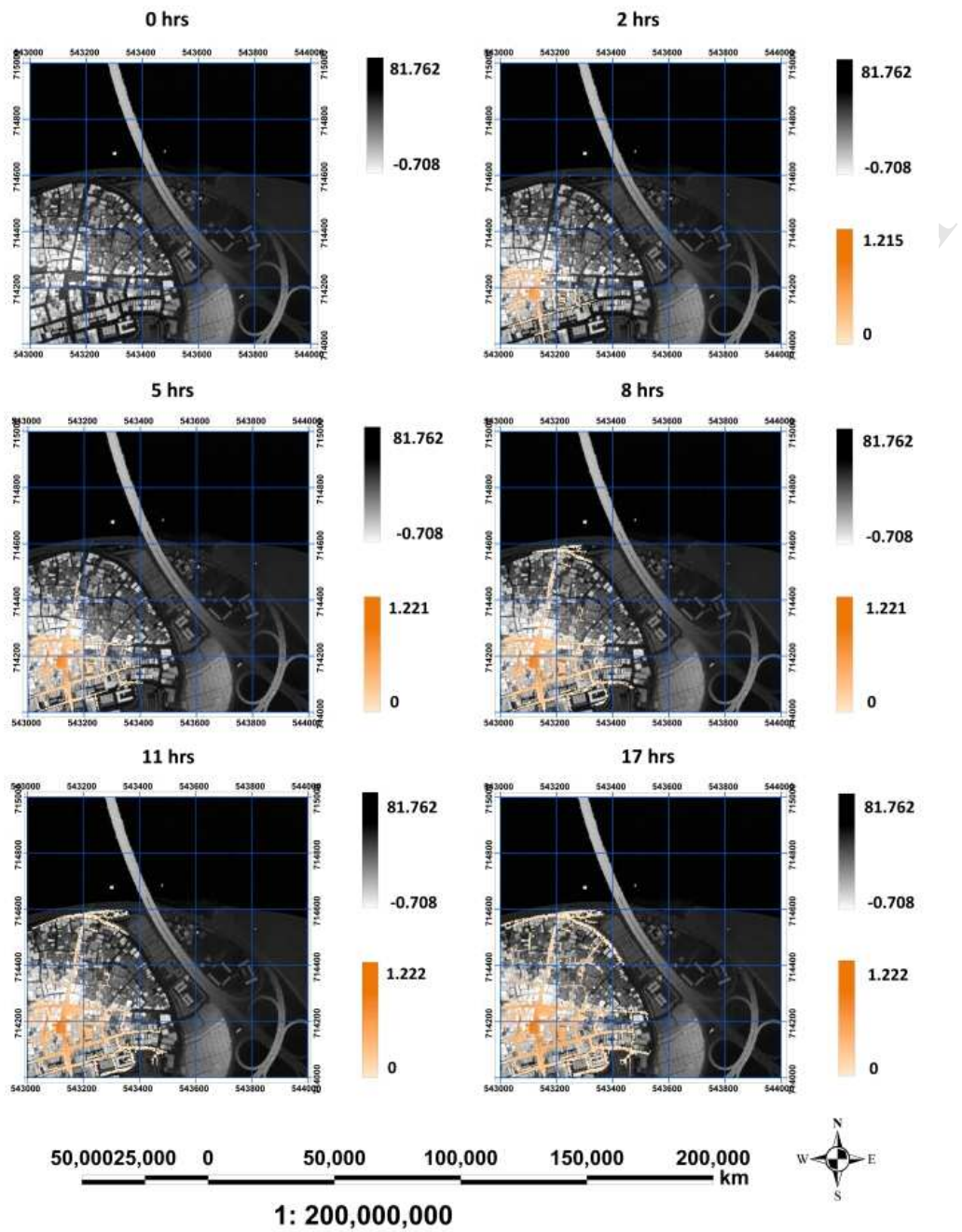


Figure 9: Simulated water depth at Lagos Island

737
738
739
740
741
742
743
744
745
746
747
748
749
750
751
752
753
754
755
756
757
758
759
760
761
762
763
764
765
766
767
768
769
770
771
772
773
774
775
776
777
778
779
780
781
782
783
784
785
786
787
788

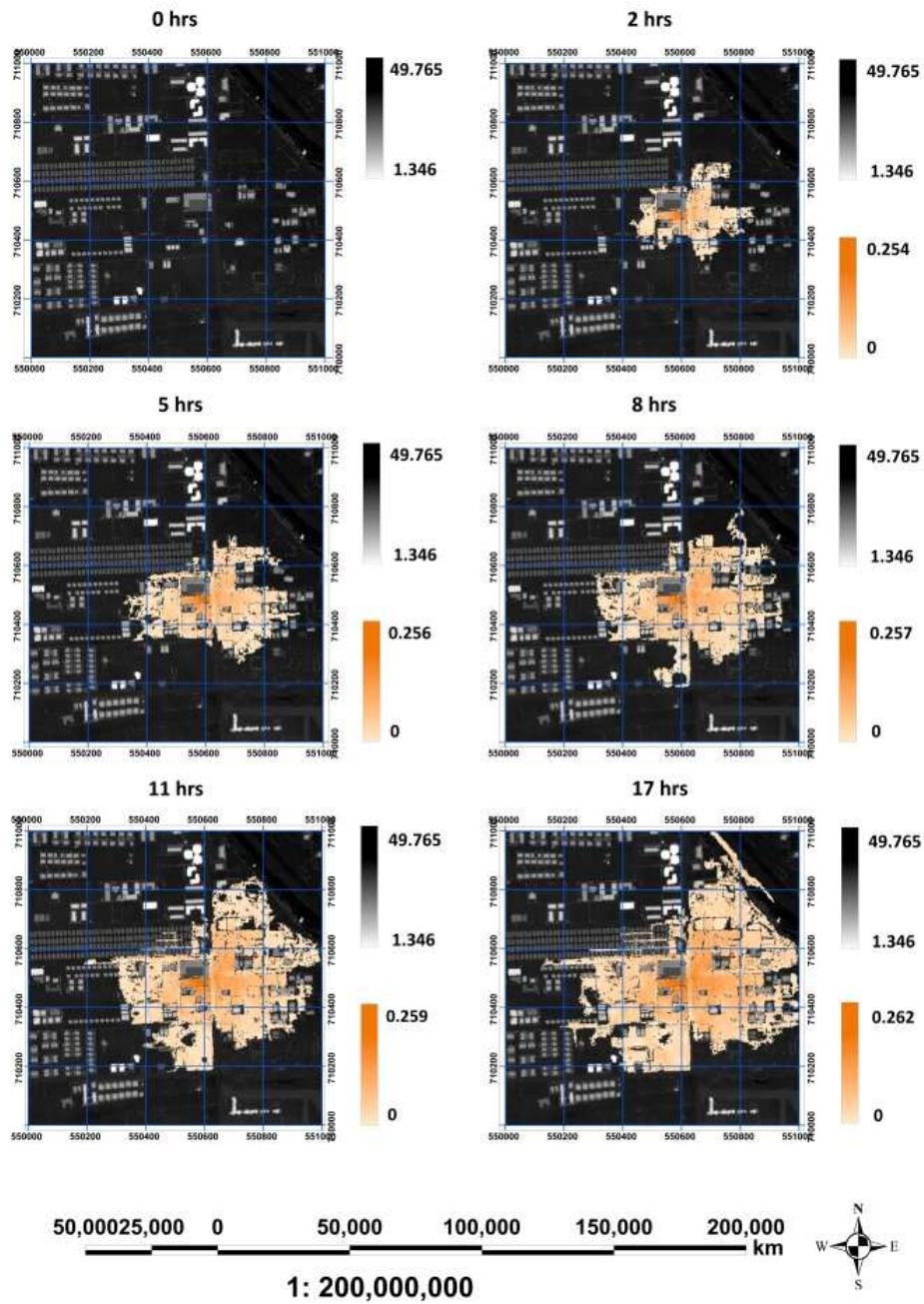


Figure 10: Simulated water depth at Castle estate

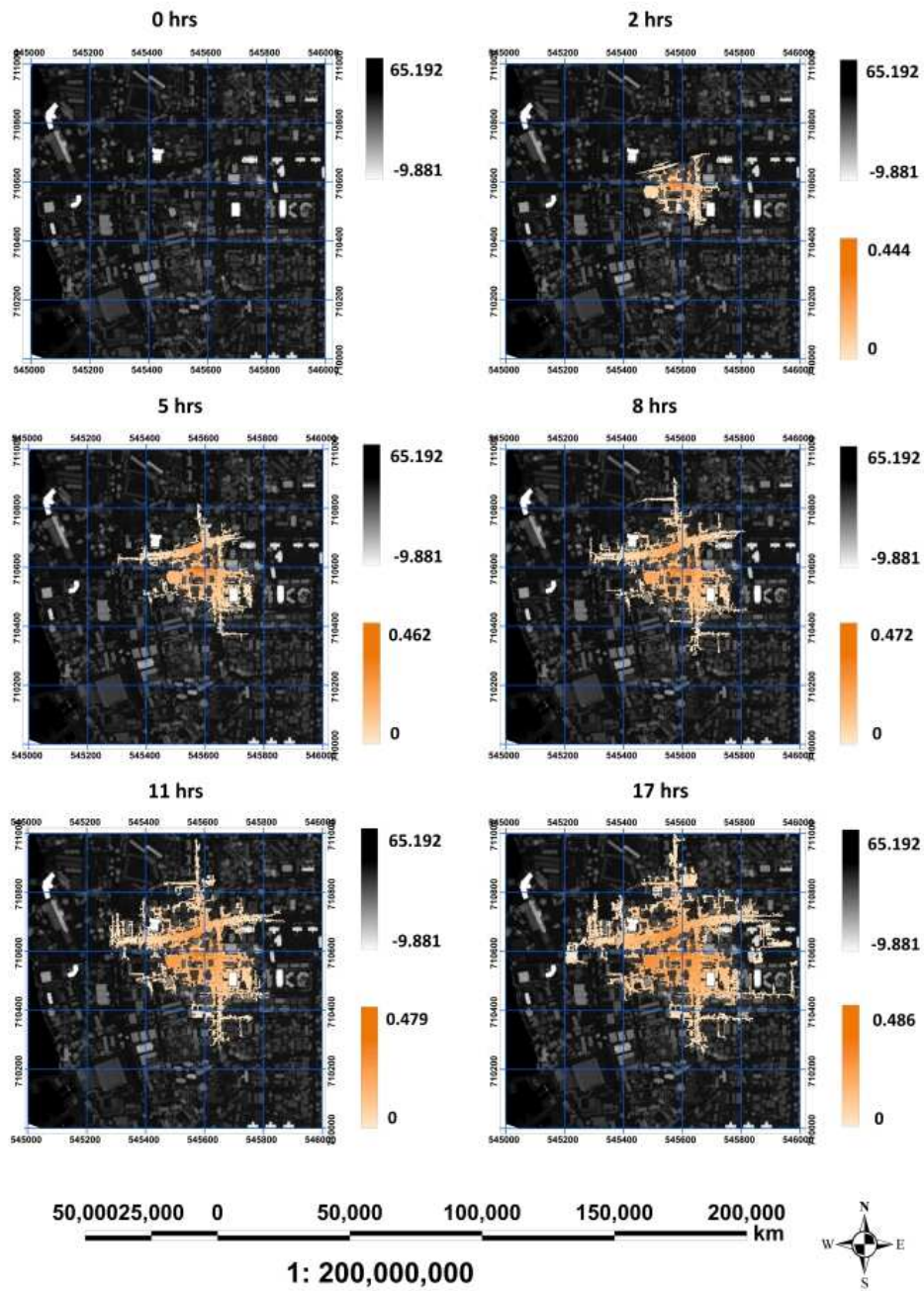


Figure 11: Simulated water depth at Victoria Island

841
842
843
844
845
846
847
848
849
850
851
852
853
854
855
856
857
858
859
860
861
862
863
864
865
866
867
868
869
870
871
872
873
874
875
876
877
878
879
880
881
882
883
884
885
886
887
888
889
890
891

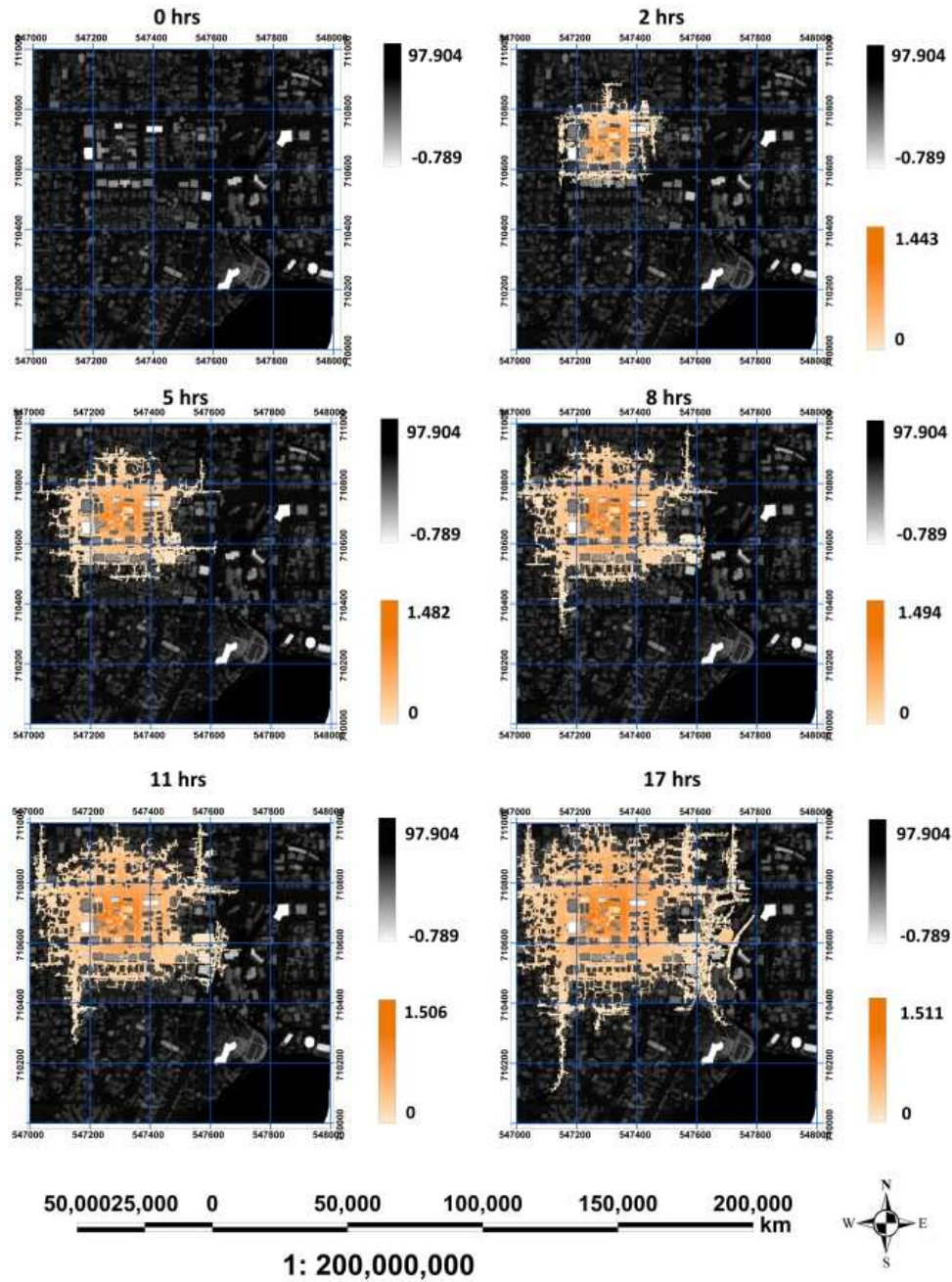
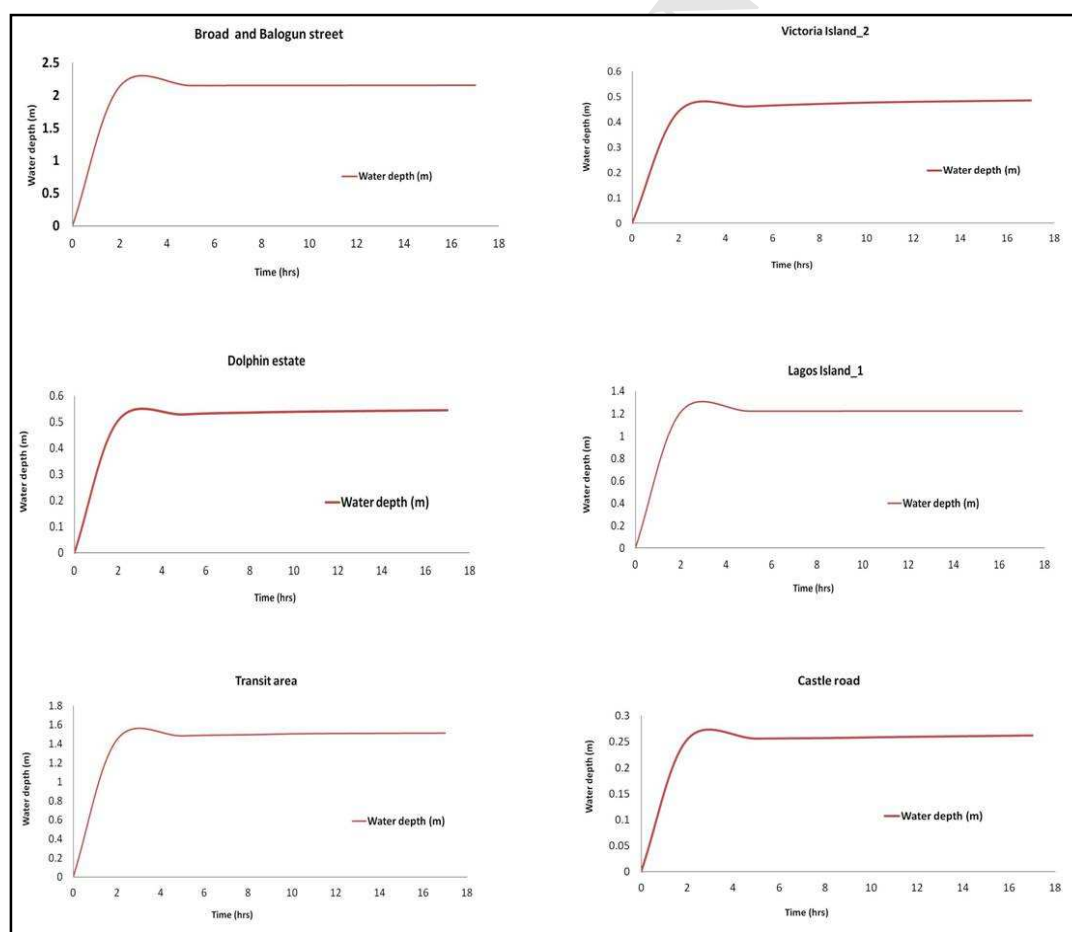


Figure 1: Adetokumbo Ademola road in Transit area, Victoria Island

892 The plots of water depth vs. time (figure 13) indicate that the simulated results are relatively
 893 stable solutions of flood hydrodynamics with respect to flood water depth and extent.
 894 Higher inundation depths were simulated around Balogun and Broad Street (2.154m),
 895 Adeyinka Oyekan Avenue (1.222m) in Lagos Island, and the area around Adetokumbo
 896 Ademola road (1.511m) in Victoria Island. This was mainly due to the relatively flat nature of
 897 the terrain at those locations. Apparently, the point with the lowest relative elevation in Lagos
 898 state, measured from 30-m horizontal, 20-m vertical resolution ASTER (Advanced Space-
 899 borne Thermal Emission and Reflection Radiometers) global DEM is 6m, and the point is
 900 located within Lagos Island. A large amount of flood water tends to accumulate in the areas
 901 from the relatively higher areas and topographic features. The maximum depths of
 902 inundation simulated for the Dolphin estate and the eastern part of Victoria Island are
 903 0.545m and 0.486m respectively. The area is characterised by built-up features that are
 904 nearly equal in elevation. There are a number of bifurcations, bridges and road junctions,
 905 around which flood water is often difficult to simulate using less efficient flood modelling
 906 methodologies (Hunter *et al.*, 2007). A low water depth (0.262m) was simulated at Castle
 907 estate towards the Lekki area and bar beach. The area is characterised by few regular blocks
 908 of building and much open spaces and lawns within which water can be stored. In all the six
 909 locations, flood water extent was extensive and covers major and minor roads, a number of
 910 built-ups including schools, residential houses and open land spaces.
 911

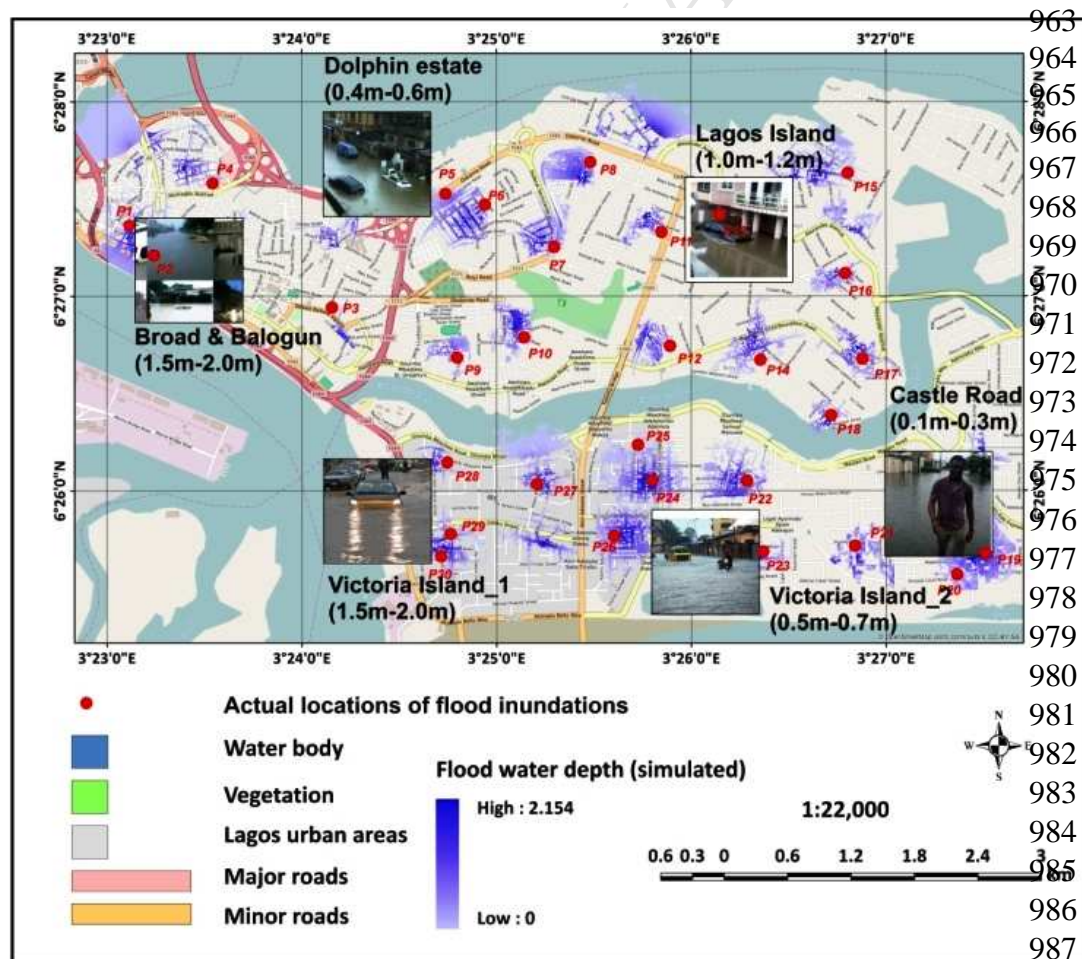


936 Figure 2: Plots of simulated water depth vs. time for the six selected locations in the study area
 937
 938
 939
 940

941 From the temporal variations of inundation depth at the chosen locations shown in figure
 942 13 above, the simulated water depth generally increased rapidly within the first two hours
 943 of the rainfall. Throughout the duration of simulation, results of simulated flood inundation
 944 show that water depth gradually increased or remained constant. It is likely that at these
 945 time intervals water is being transferred from filled higher cells (possibly the higher
 946 grounds) to lower cells (i.e. the downstream sub catchment areas).
 947

948
 949 *GFSP-1* simulates flow on downslope direction, which means that water will continue to be
 950 transferred from the principal cell to any cell with lower elevation within the neighbourhood
 951 system. Water is also transferred if a transition rule detects any available spaces within the
 952 intervening lower elevation cells in the neighbourhood system. The smooth curve in figure
 953 13 shows that the model simulation output are stable despite the absence of a stability
 954 condition, which is often used in many numerical flood models. Manning's friction
 955 coefficient used in the *GFSP-1* is important to maintain a gradual of water between cells in
 956 order to eliminate subcritical and supercritical phenomena which could render the results of
 957 the model unstable.
 958

959 To complete the validation of the *GFSP-1* model against the social media-based data, flood
 960 water depths were estimated from the six photographic, which were hotlinked to their
 961 appropriate flooded locations within the case study areas on the Lagos basemap (figure 14).
 962



988
 989

Figure 3: Thumbnails of selected photographs hotlinked to appropriate flooded locations on the Lagos basemap

990
 991
 992 The range of values estimated for maximum water depths, and their respective averages for
 993 each of the six locations are tabulated with the maximum values water depths simulated by
 994 *GFSP-1* (table 3). These values were outlined as bar charts (figure 15) and scatter plots
 995 (figure 16), to show various representations of the relationship between simulated
 996 maximum water depth values and those estimated from photographs. From the scatter
 997 plot, the Pearson correlation coefficient (r) between the simulated and estimated water
 998 depth was found to be 0.968, which is strong and indicative of robustness of the new flood
 999 model. Thus, the table and the plots show that simulated maximum values (that is values
 1000 simulated within seventeen hours flood duration) compared relatively well with averages of
 1001 estimated maximum ranges of values at the six locations, although some significant
 1002 variations occurred at Broad and Balogun street, Castle, and Lagos Island areas. This might
 1003 be due to the presence of retention ponds in those areas that were not accounted for in the
 1004 LiDAR DEM used for the simulation. Further analyses were carried out to determine the
 1005 correlation.

S/No.	Location	Maximum estimated range of water depth (m)	Average Maximum estimated range of water depth (m)	Highest simulated water depth (m)
1.	Broad and Balogun Street	1.8 - 2.0	1.9	2.154
2.	Dolphin Estate	0.4 - 0.6	0.5	0.545
3.	Lagos Island	1.0-1.2	1.1	1.222
4.	Castle Road	0.1 - 0.3	0.2	0.262
5.	Victoria Island_2	0.5 - 0.7	0.6	0.486
6.	Victoria Island	1.5 - 1.7	1.6	1.511

1006
 1007 *Table 3: Estimated maximum water depths, and their respective averages compared*
 1008 *with the maximum water depths values simulated by GFSP-1 for Lagos.*

1009
 1010
 1011
 1012 Coupling of CA and SIFDS in the new model made the simulation speed reasonably
 1013 impressive. This is somewhat an adaptive time stepping scheme which chooses a time step
 1014 for a complete iteration by comparing two time steps and choosing the minimum of the
 1015 two. On the whole, the simulation duration for *GFSP-1* is dependent of the DEM spatial
 1016 resolution. For a 2-m DEM and 17 hour (for Lagos) spells of rain lasted 3.5 hours and 5 hours
 1017 respectively on Intel(R) CPU 2.8GHz processor, 32 GB RAM and 1TB windows 10 computer.
 1018 The time could be doubled if 1-m DEM used or halved by using a 5-m DEM. Unfortunately,
 1019 scaling up the spatial grid of the DEM compromises the simulation output. However, to
 1020 restrict modelling on the basis of higher resolution DEMs, more sophisticated computer
 1021 facilities can largely improve the simulation speed of the new model.
 1022

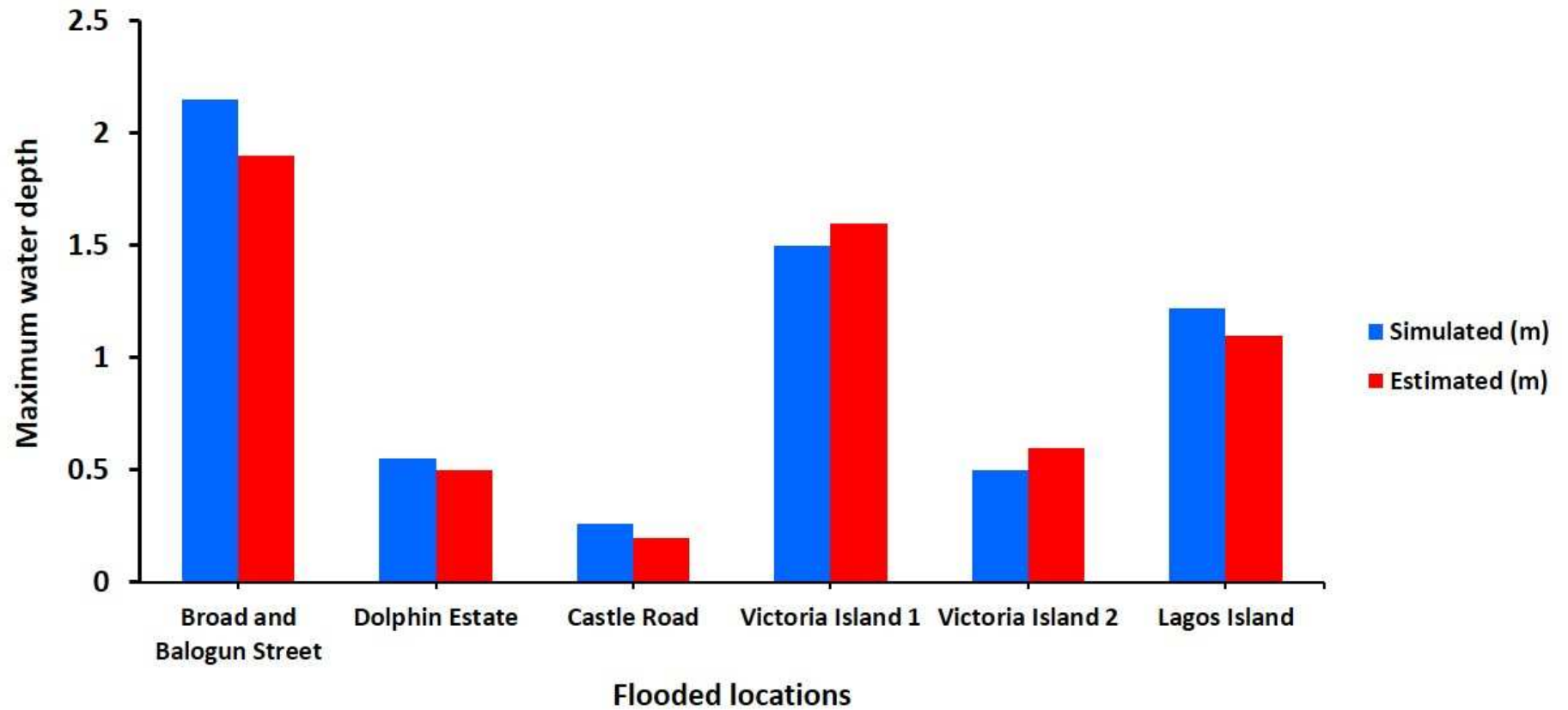


Figure 15: Bar charts showing the relationship between maximum flood water depths simulated using *GFSP-1*, compared with average water depths estimated from photographs of flooding in Lagos.

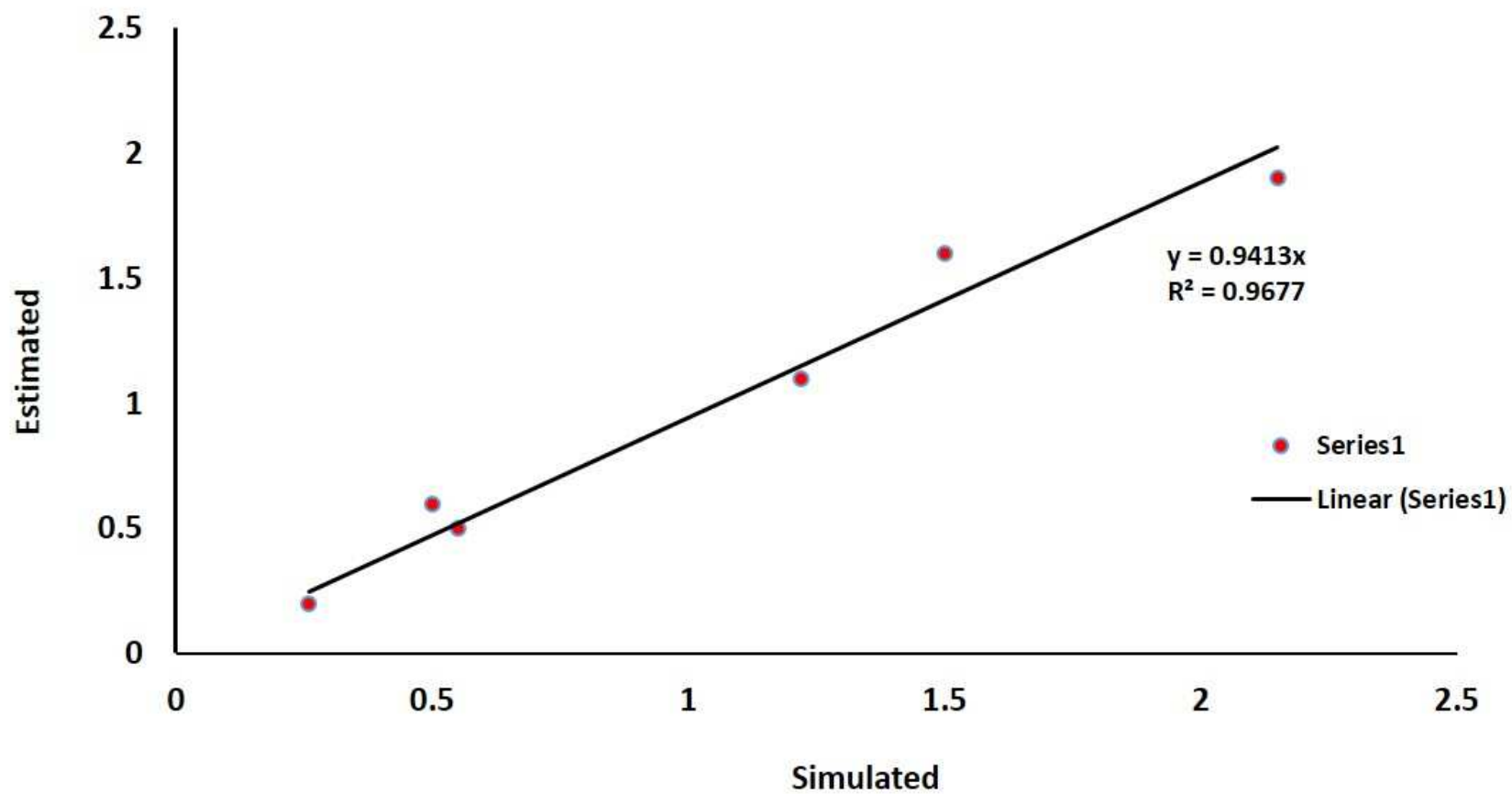


Figure 16: Scatter plots relationship between maximum flood water depths simulated using *GFSP-1*, compared with average water depths estimated from photographs of flooding in Lagos. Computed correlation coefficient is 0.968.

5. Conclusion

This study has developed an effective and efficient flood model, *GFSP-1*, to simulate urban flooding inundation for urban flood risk management. The model combines cellular automata (CA) framework and a semi-implicit finite difference scheme (SIFDS), based on the original work of Casulli (1990). Within the CA framework, a von Neumann neighborhood system defines the discrete space, whilst a set of transition rules are shown to govern the introduction of water and its movement in and out of the cell. The SIFDS is an attempt to combine the merits of explicit and implicit numerical scheme within a single numerical formulation. It is shown that the dynamic link between the CA and the SIFDS improves on the model time step. This link enables the model to maintain unconditional stability within a convenient simulation time.

This model is used to simulate the July 10th 2011 flooding in the Lagos areas of Nigeria. Using a LiDAR (Light Detection and Ranging) digital elevation model (DEM), which horizontal resolution is 2-m, rainfall amount measured during the event was input into the model, and allowed to simulate flooding within the rainfall duration which is seventeen hours. Two local government areas (LGAs) – Eti-Osa and Lagos-Island, were selected, based on the availability of the LiDAR DEM. Altogether thirty two DEMs were acquired for the simulation, and each of them measured 500m * 500m, enclosing 250, 000 cells. With such a large number of cells, the model computing time on MATLABTM platform for simulating the 17 hours rainfall event was about 4 hours, using a 6GB RAM, 500 HDD, 2.3 GHz Intel Core processing machine. This suggest a fast simulation of flooding, although this speed is subject to improvement by applying the object-oriented programming of MATLABTM, parallel computing, and by using higher processing machines.

Simulated flood inundation outputs are comparable to those recorded by the media and witnessed by local residents. These results suggest that the new model is capable of generating reliable predictions of the July 2011 urban flooding event, and this provides useful information for flood risk management in the Lagos area of Nigeria. Major innovations in the new model are: (1) the integration of SIFDS and CA, (2) the ability to run with a minimum of input data, a suitable DEM and rainfall intensity or amount and (3) outputs format that can be accessed easily using any available GIS program. Outputs from the model are written as arc grid files that can be opened easily in any GIS program.

This research is the first ever attempt to publish flood modelling procedure for the Lagos area, and this will have a significant impact in the understanding of urban flooding and flood risk management in this city. Additionally, coupling SIFDS and CA within a flood model framework is innovative in flood modelling research, and is expected to make significant contribution to the science of flood risk assessment. However, there are few uncertainties, which are being recommended for future studies. Firstly, the suitability of global DEMs to accurate prediction of flooding within the new model framework is still unknown. More testing and validation of the model using other urban inundation flood models need to be undertaken. Representation of complex urban features which influence the movement of flood water may be a major source of uncertainty to the performance of the model. This also has to be investigated in future research.

47 *Acknowledgements*

48

49 This publication is the key result of a PhD research, which has been funded by the Tertiary
50 Institutions Education Trust Fund (TETFund), a FGN/UNN academic staff intervention
51 scheme. The Surveyors Council of Nigeria (SURCON) is being acknowledged for providing
52 some supplementary grants. Data relating to the July 2011 flooding were obtained mainly
53 from previously published research and courtesy of responses from eye witnesses. The
54 anonymity of these eye witnesses has been protected in line with the ethical proviso of this
55 research. The Center for Research in Epidemiology of Disasters (CRED), Nigeria's Ministry of
56 the Environment and the Nigeria Environmental Study Action/Team (NEST) are also
57 acknowledged. Previous works in the area of flood modelling, especially the original work of
58 Professor Vincenzo Casulli, are equally acknowledged, and so are the anonymous reviewers,
59 and the editor of this journal.

60

61

62 **References**

63

64 Adelekan, O. (2010). Vulnerability of poor urban coastal communities to flooding in Lagos,
65 Nigeria. *Environment and Urbanization*, 22, 433-450.

66

67 Adelekan, I. O. (2015). Flood risk management in the coastal city of Lagos, Nigeria. *Journal of*
68 *Flood Risk Management*. DOI: 10.1111/jfr3.12179.

69

70 Aderogba, K. A. (2012). Global warming and challenges of floods in Lagos metropolis,
71 Nigeria. *Academic Research International*, 2(1), 448-468.

72

73 Akanni, O., & Bilesanmi, L. (2011, July 20). Flood: Lagos residents forced to relocate
74 Drowning teenager rescued in Vanguard: Towards a Better Life for the People. *Lagos:*
75 *Vanguard Media Limited*, p. 20.

76

77 Ajibade, I., McBean, G., & Bezner-Kerr, R. (2013). Urban flooding in Lagos, Nigeria: Patterns
78 of vulnerability and resilience among women. *Global Environmental Change*, 23, 1714-1725.

79

80 Alexander, D. E. (2014). Social media in disaster risk reduction and crisis management.
81 *Science and Engineering Ethics*, 20(3), 717-733.

82

83 Anees, M. T., Abdullah, K., Nawawi, M. N. M., Ab Rahman, N. N. N., Piah, A. R. M., Zakaria,
84 N. A., Syakir, M.I., & Omar, A. M. (2016). Numerical modeling techniques for flood analysis.
85 *Journal of African Earth Sciences*, 124, 478-486.

86

87 Bazilevs, Y., & Hughes, T. J. (2007). Weak imposition of Dirichlet boundary conditions in fluid
88 mechanics. *Computers & Fluids*, 36(1), 12-26.

89

90 Casulli, V. (1990). Semi-implicit finite difference methods for the two-dimensional shallow
91 water equations. *Journal of Computational Physics*, 86(1), 56-74.

92

93 Casulli, V., & Stelling, G. S. (2013). A semi-implicit numerical model for urban drainage
94 systems. *International Journal for Numerical Methods in Fluids*, 73(6), 600-614.

95

96 Chen, A. S., Evans, B., Djordjević, S., & Savić, D. A. (2012). Multi-layered coarse grid
97 modelling in 2D urban flood simulations. *Journal of Hydrology*, 470, 1-11.

98

99 Chen, C. L. (1983). Rainfall intensity-duration-frequency formulas. *Journal of Hydraulic*
100 *Engineering*, 109(12), 1603-1621.

101

102 Cherqui, F., Belmeziti, A., Granger, D., Sourdril, A., & Le Gauffre, P. (2015). Assessing urban
103 potential flooding risk and identifying effective risk-reduction measures. *Science of the Total*
104 *Environment*, 514, 418-425.

105

106 Chow, V.T., Maidment, D.R., & Mays, L.W. (1988). *Applied Hydrology*. New York: McGraw-
107 Hill.

108

- 109 Cirbus, J., & Podhoranyi, M. (2013). Cellular automata for the flow simulations on the earth
110 surface, optimization computation process. *Applied Mathematics & Information Sciences*,
111 7(6), 2149.
112
- 113 Costabile, P., & Macchione, F. (2015). Enhancing river model set-up for 2-D dynamic flood
114 modelling. *Environmental Modelling & Software*, 67, 89-107.
115
- 116 de Albuquerque, J. P., Herfort, B., Brenning, A., & Zipf, A. (2015). A geographic approach for
117 combining social media and authoritative data towards identifying useful information for
118 disaster management. *International Journal of Geographical Information Science*, 29(4),
119 667-689.
120
- 121 Djordjević, S., Butler, D., Gourbesville, P., Mark, O., & Pasche, E. (2011). New policies to deal
122 with climate change and other drivers impacting on resilience to flooding in urban areas: the
123 CORFU approach. *Environmental Science & Policy*, 14(7), 864-873.
124
- 125 Dumbser, M., & Casulli, V. (2013). A staggered semi-implicit spectral discontinuous Galerkin
126 scheme for the shallow water equations. *Applied Mathematics and Computations*, 219,
127 8057-8077.
128
- 129 Dumbser, M., Iben, U., & Ioriatti, M. (2015). An efficient semi-implicit finite volume method
130 for axially symmetric compressible flows in compliant tubes. *Applied Numerical
131 Mathematics*, 89, 24-44.
132
- 133 Engelen, G., White, R., Uljee, I., & Drazan, P. (1995). Using cellular automata for integrated
134 modelling of socio-environmental systems. *Environmental Monitoring and Assessment*,
135 34(2), 203-214.
136
- 137 Etuonovbe A. K. (2011). The devastating effect of flooding in Nigeria. In FIG Working Week.
138 2011, May. Accessed 10 March 2015; Available at:
139 http://www.fig.net/pub/fig2011/papers/ts06j/ts06j_etuonovbe_5002.pdf
140
- 141 Fohringer, J., Dransch, D., Kreibich, H., & Schröter, K. (2015). Social media as an information
142 source for rapid flood inundation mapping. *Natural Hazards and Earth System Sciences*,
143 15(12), 2725-2738.
144
- 145 Ghimire, B., Chen, A. S., Guidolin, M., Keedwell, E. C., Djordjević, S., & Savić, D. A. (2013).
146 Formulation of a fast 2D urban pluvial flood model using a cellular automata approach.
147 *Journal of Hydroinformatics*, 15(3), 676-686.
148
- 149 IFRC (International Federation of Red Cross and Red Crescent) (2011): Nigeria: Floods – July,
150 available at: <http://reliefweb.int/disaster/fl-2012-000138-nga> (last access: 10 March 2015).
151
- 152 Kaźmierczak, A., & Cavan, G. (2011). Surface water flooding risk to urban communities:
153 Analysis of vulnerability, hazard and exposure. *Landscape and Urban Planning*, 103(2), 185-
154 197.
155

- 156
157 Kim, D., Sun, Y., Wendi, D., Jiang, Z., Liang, S. Y., & Gourbesville, P. (2018). Flood Modelling
158 Framework for Kuching City, Malaysia: Overcoming the Lack of Data. In *Advances in*
159 *Hydroinformatics* (pp. 559-568). Springer, Singapore.
- 160
161 Kulkarni, A. T., Mohanty, J., Eldho, T. I., Rao, E. P., & Mohan, B. K. (2014). A web GIS based
162 integrated flood assessment modeling tool for coastal urban watersheds. *Computers &*
163 *Geosciences*, 64, 7-14.
- 164
165 Lagos State Government (LSG). (2012). Abstract of Local Government Statistics, Lagos: Lagos
166 Bureau of Statistics, Ministry of Economic Planning and Budget Secretariat, Alausa, Ikeja.
- 167
168 Latonero, M., & Shklovski, I. (2011). Emergency management, Twitter, and social media
169 evangelism. *International Journal of Information Systems for Crisis Response and*
170 *Management*, 3(4), 67-86.
- 171
172 Liu, L., Liu, Y., Wang, X., Yu, D., Liu, K., Huang, H., & Hu, G. (2015). Developing an effective 2-
173 D urban flood inundation model for city emergency management based on cellular
174 automata. *Natural Hazards and Earth System Sciences* 15, 381–391.
- 175
176 Martin, N., & Gorelick, S. M. (2005). MOD_FreeSurf2D: A MATLAB surface fluid flow model
177 for rivers and streams. *Computers and Geosciences*, 31(7), 929-946.
- 178
179 Nkwunonwo, U. C., Malcolm, W., & Brian, B. (2015). Flooding and Flood Risk Reduction in
180 Nigeria: Cardinal Gaps. *Journal of Geography & Natural Disasters*, 5(1), 1-12.
- 181
182 Nkwunonwo, U. C., Whitworth, M., & Baily, B. (2016). Review article: A review and critical
183 analysis of the efforts towards urban flood risk management in the Lagos region of Nigeria.
184 *Natural Hazards and Earth System Sciences*, 16(2), 349-369.
- 185
186 Oyinloye, M., Olamiju, I., & Adekemi, O. (2013). Environmental impacts of flooding on
187 Kosofo local government area of Lagos state, Nigeria: A GIS perspective. *Journal of*
188 *Environmental and Earth Science* 3(5), 57-66.
- 189
190 Perales-Momparler, S., Andrés-Doménech, I., Hernández-Crespo, C., Vallés-Morán, F.,
191 Martín, M., Escuder-Bueno, I., & Andreu, J. (2017). The role of monitoring sustainable
192 drainage systems for promoting transition towards regenerative urban built environments:
193 A case study in the Valencian region, Spain. *Journal of Cleaner Production*, 163, S113-S124.
- 194
195 Smith, K. (2013). *Environmental hazards: assessing risk and reducing disaster*. Routledge.
- 196
197 Smith, L., Liang, Q., James, P., & Lin, W. (2015). Assessing the utility of social media as a data
198 source for flood risk management using a real-time modelling framework. *Journal of Flood*
199 *Risk Management*.
- 200
201 Teng, J., Jakeman, A. J., Vaze, J., Croke, B. F., Dutta, D., & Kim, S. (2017). Flood inundation
202 modelling: A review of methods, recent advances and uncertainty analysis. *Environmental*
203 *Modelling & Software*, 90, 201-216.

- 204
205 Von Neumann, J. (1951). The general and logical theory of automata. *Cerebral Mechanisms*
206 *in Behaviour*, 1(41), 1-2.
207
- 208 Wahle, J., Neubert, L., Esser, J., & Schreckenberg, M. (2001). A cellular automaton traffic
209 flow model for online simulation of traffic. *Parallel Computing*, 27(5), 719-735.
210
- 211 Wójcik, R., & Buishand, T. A. (2003). Simulation of 6-hourly rainfall and temperature by two
212 resampling schemes. *Journal of Hydrology*, 273(1-4), 69-80.
213
- 214 Yamamoto, K., Kokubo, S., & Nishinari, K. (2007). Simulation for pedestrian dynamics by
215 real-coded cellular automata (RCA). *Physica A: Statistical Mechanics and its Applications*,
216 379(2), 654-660.
217
- 218 Zevenbergen, C., Veerbeek, W., Gersonius, B., & Van Herk, S. (2008). Challenges in urban
219 flood management: travelling across spatial and temporal scales. *Journal of Flood Risk*
220 *Management*, 1(2), 81-88.
221
- 222 Zevenbergen, L.W., & Throne, C.R. (1987). Quantitative analysis of land surface topography.
223 *Earth Surface Processes and Landforms*, 12, 47-56.
224
225